The Astrophysical Journal, 621:L33–L36, 2005 March 1

COMPETITION BETWEEN CO AND N_2 DESORPTION FROM INTERSTELLAR ICES

K. I. Öberg,[1,2] F. van Broekhuizen,[1] H. J. Fraser,[1] S. E. Bisschop,[1] E. F. van Dishoeck,[1] and S. Schlemmer[1]

Received 2004 November 8; accepted 2005 January 18; published 2005 February 2

ABSTRACT

Millimeter observations of pre- and protostellar cores show that the abundances of the gas-phase tracer molecules, $C^{18}O$ and N_2H^+, anticorrelate with each other and often exhibit "holes" where the density is greatest. These results are reasonably reproduced by astrochemical models, provided that the ratio between the binding energies of N_2 and CO, R_{BE}, is taken to be between 0.5 and 0.75. This Letter is the first experimental report of the desorption of CO and N_2 from layered and mixed ices at temperatures relevant to dense cores, studied under ultrahigh vacuum laboratory conditions using temperature programmed desorption. From control experiments with pure ices, $R_{BE} = 0.923 \pm 0.003$, given $E_b(N_2\text{-}N_2) = 790 \pm 25$ K and $E_b(CO\text{-}CO) = 855 \pm 25$ K. In mixed (CO:N_2 = 1:1) and layered (CO above or below N_2) ice systems, both molecules become mobile within the ice matrix at temperatures as low as 20 K and appear miscible. Consequently, although a fraction of the deposited N_2 desorbs at lower temperatures than CO, up to 50% of the N_2 molecules leave the surface as the CO itself desorbs, a process not included in existing gas-grain models. This codesorption suggests that for a fraction of the frozen-out molecules, R_{BE} is unity. The relative difference between the CO and N_2 binding energies as derived from these experiments is therefore significantly less than that currently adopted in astrochemical models.

Subject headings: astrochemistry — infrared: ISM — ISM: molecules — methods: laboratory

Online material: color figure

1. INTRODUCTION

Dense molecular clouds are the starting point in our understanding of star formation. These regions evolve toward characteristically cold ($\lesssim$10 K), centrally concentrated, prestellar cores, which then collapse to form protostars. The fundamental properties of these cores are determined almost exclusively from observations of optically thin gas-phase tracers. However, as cores evolve toward the collapse phase, densities increase and the timescales for volatile gas-phase molecules to deplete onto grains become shorter than the age of the core (e.g., Caselli et al. 1999; Walmsley et al. 2004). Of the critical processes governing chemical differentiation in starless cores that are not yet well understood, a key issue is the relative freezeout and desorption rates of CO and N_2 (Bergin & Langer 1997, hereafter BL97).

$C^{18}O$ accurately traces the distribution of material in cold, dense cores, except in regions of high extinction ($A_v \gtrsim 10$ mag; e.g., Kramer et al. 1999). When CO becomes frozen out onto the surfaces of cold dust grains, a corresponding drop is observed in the gas-phase $C^{18}O$ abundance (e.g., Bergin et al. 2001; Tafalla et al. 2002; Pagani et al. 2005), and solid ^{12}CO is detected (e.g., Chiar et al. 1998; Whittet et al. 1998 and references therein). Unfortunately, N_2 is not directly observable in the gas phase, and the vibrational band strength of solid $^{14}N_2$ is around 5 orders of magnitude lower than the corresponding band strength of ^{12}CO, making its detection in interstellar ices impossible (Sandford et al. 2001). The N_2 gas abundance is therefore inferred from observations of its chemical "daughters," such as N_2H^+.

The detailed chemical network of N_2H^+ formation and destruction is described in detail by Jørgensen et al. (2004), showing that the chemistries of CO, N_2, N_2H^+, HCO^+, and H_3^+ are intimately entwined. N_2H^+ is considered a more suitable gas-phase tracer than $C^{18}O$ because its abundance can remain constant when CO is depleted (Bergin et al. 2001; Tafalla et al. 2002; Di Francesco et al. 2004; Pagani et al. 2005; Jørgensen 2004). However, depletion of N_2H^+ (and thus N_2) has been detected within the densest regions of the prestellar B68 dark cloud (Bergin et al. 2002), around the Class 0 source IRAM 04191 +1522 (Belloche & André 2004), within starless cores in L183 (Pagani et al. 2005), and in a range of sources in Oph A (Di Francesco et al. 2004).

In gas-grain models, the relative abundances of gas-phase CO and N_2 are governed by the balance of the freezeout timescales—which depend mostly on density—and the desorption timescales—which depend mostly on the grain temperature, binding energies, and desorption kinetics. Models reasonably assume that for both molecules, and at grain temperatures lower than 10–15 K, all sticking probabilities are very close to 1, so the freezeout timescales are identical for a given grain density. By using first-order desorption kinetics, with preexponential factors, $\nu_0 \approx 10^{12}$ s^{-1}, models can reproduce the N_2H^+ and CO observations by assuming that the difference between the desorption rates of CO and N_2 is a direct function of the ratios between their binding energies, $R_{BE} = E_b(N_2\text{-}N_2)/E_b(CO\text{-}CO)$. For example, BL97 set R_{BE} at 0.65, based on the ab initio calculations of Sadlej et al. (1995) and assuming $E_b(CO\text{-}CO) = 960$ K. Subsequently, Bergin et al. (2002) used an extension of the BL97 chemical model to reproduce their observations of N_2H^+ in B68, with initial values for the binding energies of CO-CO and N_2-N_2 of 1210 and 750 K, respectively ($R_{BE} = 0.62$), although best fits to the emission spectra were actually obtained with $E_b(N_2\text{-}N_2) = 900$ K ($R_{BE} = 0.75$). Conversely, Aikawa et al. (2003) assume that the value R_{BE} is even lower than that used in BL97. The range of binding energies applied in each case arises owing to a lack of relevant laboratory data in the literature.

To accurately model the entire CO-N_2 gas-grain system, a minimum of five binding energies need to be known, namely, those for N_2-N_2, CO-N_2, H_2O-N_2, CO-CO, and H_2O-CO, together with a knowledge of the order of reaction and preexponential factor in the rate equations describing the desorp-

[1] Raymond and Beverly Sackler Laboratory for Astrophysics at Leiden Observatory, Postbus 9513, 2300 RA, Leiden, Netherlands; fraser@strw.leidenuniv.nl.

[2] Current address: Division of Geological and Planetary Sciences, California Institute of Technology, Mail Stop 150-21, Pasadena, CA 91125.

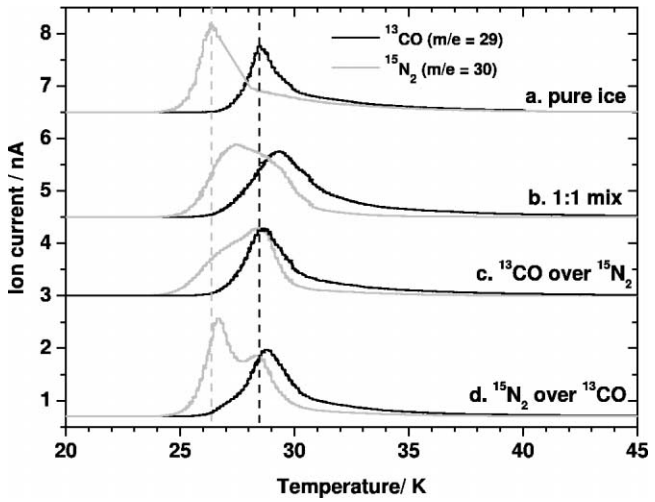

FIG. 1.—TPD spectra of (*a*) pure CO (40 L) and N_2 (40 L), (*b*) an intimately mixed equimolar CO-N_2 ice (80 L total exposure), (*c*) an N_2 layer (40 L) over a CO layer (40 L), and (*d*) a CO layer (40 L) over an N_2 layer (40 L). The ^{13}CO ($m/e = 29$) traces are in black; $^{15}N_2$ ($m/e = 30$) traces are in gray. The heating rate is 0.1 K minute^{-1}. The two dashed lines are superposed on the plot to show the positions of the desorption peaks of the 40 L pure samples of N_2 (*gray*) and CO (*black*).

tion processes. In light of these needs, the best laboratory analog mimicking the interstellar case would be the tertiary ice system, N_2-CO-H_2O, where CO and N_2 are sequentially or coadsorbed on a preexisting porous H_2O-ice layer. One such qualitative study has been made under high-vacuum conditions showing that, after codeposition of all three molecules (producing a mixed ice), more CO than N_2 becomes trapped in H_2O ices (Notesco & Bar-Nun 1996). However, no mention is made of the kinetics or binding energies in the paper, and as its focus was CO and N_2 in cometary systems, the ice surface was held at temperatures in excess of 40–50 K, not relevant to cold, prestellar cores.

It is known from observations that in many pre- and protostellar cores, up to 90% of the CO is frozen out in a distinct layer separated from the H_2O ice (Tielens et al. 1991; Pontoppidan et al. 2003). If N_2 freezes out subsequent to CO, it is likely to form an ice layer *above* the CO ice, creating segregated N_2/CO ices, or if CO continues to accrete to the grain, a mixed CO-N_2 ice. Consequently, the interplay between CO and N_2 during their desorption from binary CO-N_2 ice systems is equally relevant.

2. EXPERIMENTAL PROCEDURE

The apparatus used here, CRYOPAD (F. van Broekhuizen et al. 2005, in preparation), is very similar to the other Leiden instrument, SURFRESIDE, described in detail elsewhere (Fraser & van Dishoeck 2004). Briefly, the experiments were performed in an ultrahigh vacuum chamber, reaching base pressures of better than 1×10^{-10} mbar. At the center of the chamber is a gold-coated copper substrate, mounted in close thermal contact with a closed-cycle He cryostat, which cools the whole substrate to 12 K. The system temperature is monitored with two thermocouples, one mounted on the substrate, the second by the heater element. Ices are grown in situ, by exposing the cold substrate to a steady flow of gas, directed along the surface normal. Desorption is induced by linear heating of the substrate (and ice sample): during film growth or temperature programmed desorption (TPD), gases liberated from the surface are monitored using a quadrupole mass spectrometer (Pfeiffer Prisma). TPD is a well-established method in surface science for determining surface-adsorbate binding energies (e.g., Attard & Barnes 1998, p. 72; Woodruff & Delchar 1994).

Mixed (CO:N_2) and layered (N_2/CO) ice morphologies were studied. For completeness, control experiments were conducted on pure CO and pure N_2 ice films. Previous spectroscopic studies have shown that almost equal amounts of N_2 and CO can be frozen out onto interstellar grains without detectably affecting the line profile of the solid-CO vibrational band (Elsila et al. 1997). Therefore, the three ice morphologies were studied in equimolar ratios. To enable the two molecules to be discriminated from each other (and the background signal) with mass spectrometry, isotopes of both molecules were used, i.e., ^{13}CO (Cambridge Isotopes, Inc., 99%), $m/e = 29$, and $^{15}N_2$ (Cambridge Isotopes, Inc., 98%), $m/e = 30$.

In the pure and layered ice morphologies, the gases were used as supplied; to form the mixed ices, a 1:1 gas mixture of ^{13}CO:$^{15}N_2$ was pre-prepared then mounted on the chamber. The dosing rate for ice-film growth was set prior to cooling the sample, by sequentially backfilling the chamber with the gas(es) of interest, to a pressure of around 1×10^{-8} mbar, equivalent to an ion reading on the mass spectrometer of 7.5×10^{-10} A for both $^{15}N_2$ and ^{13}CO. After cooling the substrate to 12 K, the ice films were grown by opening the preset flow valve for exposure times equivalent to a dose of 40 langmuirs (L) per sample gas (where 1 L $\approx 1 \times 10^{-6}$ torr s), i.e., the number of molecules of each gas deposited on the surface is equivalent to the number of molecules in 40 monolayers of a nonporous condensed solid, assuming 1×10^{15} molecules cm^{-2}. The value of 40 L was chosen for two reasons: First, it is the upper limit to the number of equivalent monolayers of pure CO ice condensed on grains on lines of sight to low-mass stars, as determined by Pontoppidan et al. (2003). Second, additional experiments (not shown here) indicate that at this ice thickness the behavior of the sample is substrate-independent (S. E. Bisschop et al. 2005, in preparation). Finally, the ice sample was warmed from 12 to 80 K at a rate of 0.1 K minute^{-1} while the desorbing gases were monitored at the mass spectrometer.

3. RESULTS

The TPD spectra from each of the ice systems are shown in Figure 1. Equal amounts of either N_2 (*gray traces*) or CO (*black traces*) contribute to the TPD signal such that the integrated area under each TPD curve is constant to within $\pm 5\%$ and the desorption characteristics of the different ice morphologies can be compared directly.

Pure ices.—In Figure 1*a*, the data from 40 L exposure pure CO and N_2 ices are overlaid. It is clear that N_2 desorbs at lower temperatures than CO. TPD data from layers of higher and lower exposures (not shown) confirm that, at 40 L exposure, the desorption kinetics of N_2 and CO are zeroth order, like those of H_2O, i.e., the preexponential factor will typically have a value between 10^{28} and 10^{32} molecules cm^{-2} s^{-1} (Fraser et al. 2001; Collings et al. 2003a), and the desorption rate is independent of the amount of CO or N_2 adsorbed at the surface. If we assume the enthalpy of adsorption and desorption in these systems are equal, the mean desorption energies (in units of kelvins) are equivalent to the mean binding energy and can be approximately estimated from the TPD peak position (Attard & Barnes 1998, p. 72),

$$E_b = T_{\rm peak} \times 30.068, \quad (1)$$

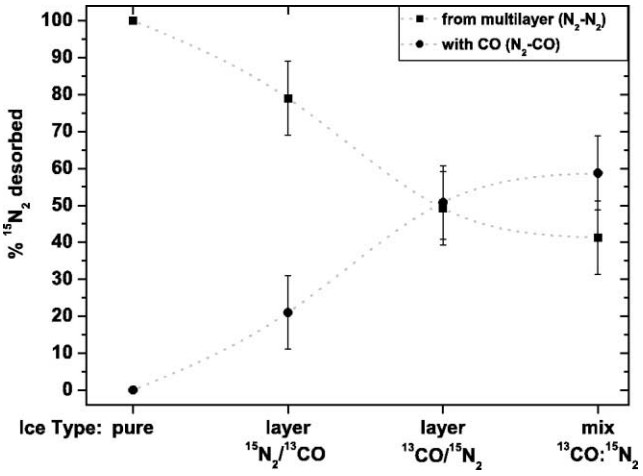

FIG. 2.—Fraction of N_2 desorbing from pure and mixed ice environments in each of the ice systems studied as a percentage of the total N_2 desorbed at the end of each experiment. See text for details.

giving $E_b(N_2\text{-}N_2) = 790 \pm 25$ K and $E_b(\text{CO-CO}) = 855 \pm 25$ K, respectively ($R_{BE} = 0.923 \pm 0.003$). The error bars on E_b arise from a conservative estimate of the range in which T_{peak} actually lies, given that in zeroth-order desorption the TPD peak position shifts to higher temperatures and higher intensities as the surface coverage increases. It should be stressed that the mean desorption energies quoted throughout this Letter are *estimates* and the absolute values of E_b can only be accurately determined from kinetic models of the system, the subject of a future publication. Consequently, the error bars are larger than those obtained from the TPD peak positions alone, which can be read more precisely and are reproducible to ± 0.05 K for identical surface coverages. Within experimental error, our E_b(CO-CO) is consistent with that reported by Collings et al. (2003a) of 830 ± 20 K. Our values are also close to the sublimation enthalpies of N_2 and CO determined from IUPAC accredited data (Lide 2002), i.e., 756 ± 5 K and 826 ± 5 K, respectively, giving a ratio $R_{BE} = 0.915$ (upper limit = 0.923, lower limit = 0.903).

Layered ices.—In Figures 1*c* and 1*d*, TPD data from layered CO-N_2 ices are shown. As with the pure CO-ice samples, the onset of CO desorption occurs at around 26 K, and over 95% of the CO has desorbed by 31–32 K. It seems that CO only desorbs from a CO-dominated environment, although in comparison to the pure CO sample the presence of N_2 may result in a small increase in the range of binding sites from which desorption occurs, accounting for the slight broadening of the TPD profile. The mean desorption energy of CO molecules from the ice, E_b(CO-CO), is 855 ± 25 K, and like the pure CO ice, the desorption kinetics of CO in layered CO-N_2 ice systems follow zeroth-order kinetics.

Although a significant fraction of the N_2 desorbs at lower temperatures than CO, i.e., 24–27.5 K, a second peak is clearly visible in the desorption profile of the layered ices, corresponding to codesorbing N_2. This is interpreted as some fraction of the N_2 molecules becoming mobile and diffusing into the CO ice, where they become mixed. To establish the relative fractions of N_2 desorbing from each environment, a simple analysis was undertaken. The pure N_2 TPD trace (Fig. 1*a*) was scaled to fit the leading edge of each of the other N_2 TPD traces (Figs. 1*b*–1*d*), then subtracted. The integrated area under the scaled, pure-N_2 trace was then attributed to N_2 molecules desorbing from a pure ice environment, and the integrated area under the remaining curve to a mixed ice environment, under the assumption that

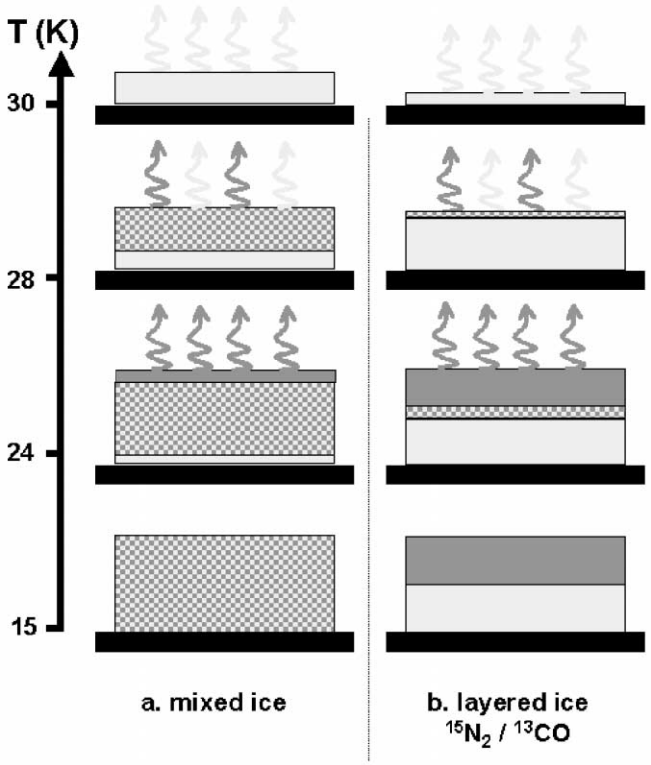

FIG. 3.—Summary of the desorption behavior of CO and N_2 within astronomically relevant ice systems. Pure CO and N_2 are represented by light gray and dark gray shading, respectively; mixed ice regions are checkered. Desorption is indicated by the wiggly arrows. (*a*) Mixed ice: The ice components begin segregating as soon as the ice is heated, forming layers of CO and N_2, below and above the remaining ice mixture. Further heating leads to the onset of N_2 desorption from the segregated N_2 layer and then codesorption of CO and N_2, until all the N_2 has desorbed. Finally, only CO is desorbing from the surface. (*b*) Layered ice: As the N_2/CO layered ice is heated, the majority of N_2 molecules desorb directly from the upper surface of the N_2 multilayer. From ≈20 K, the diffusion of CO and/or N_2 across the layer interface leads to mixing between the two ice layers, and a fraction of the N_2 molecules subsequently codesorb with the CO molecules. [*See the electronic edition of the Journal for a color version of this figure*.]

each TPD trace is a linear combination of these two contributions. The results of this analysis are shown in Figure 2, where the error bars arise from the uncertainty in the initial scaling of the pure N_2 trace. The fraction of N_2 desorbing from the pure and mixed ice environments depends intrinsically on the initial morphology of the ice system. If N_2 is deposited above an existing CO ice layer, the majority of N_2 molecules do desorb prior to CO, whereas when N_2 is deposited below a CO layer about 50% of the N_2 molecules codesorb with the CO. This implies that the desorption kinetics are unchanged between layered and pure ice systems (i.e., still zeroth order) and R_{BE} is unaltered, i.e., $R_{BE} = 0.923 \pm 0.003$. The value $E_b(\text{CO-}N_2)$ is determined from the codesorbing fraction of N_2, i.e., $\approx 855 \pm 25$ K, i.e., $R_{BE} = 1$, although further differential N_2 exposure experiments are required to confirm this value.

CO-N_2 *ice mixture*.—In Figure 1*b*, the mixed ice CO TPD data are broadened and shifted to higher temperatures in comparison to the pure CO ice or layered ice systems. From the leading edge of the CO TPD trace, plus evidence from thickness-dependent studies (not shown), it appears that the CO desorption is hindered by the presence of N_2. This results in a small shift in the TPD peak position, commensurate with a rise in the mean desorption energy of the CO molecules, i.e., $E_b(\text{CO-CO}) = 885 \pm 25$ K. This implies that the majority of the CO molecules in a mixed ice desorb from slightly different binding environ-

ments to those from which desorption occurs in pure and layered ice systems. Figure 2 shows that at least 50% of the N_2 originally deposited in the mixture actually codesorbs with the CO. The remaining N_2 desorbs from an environment resembling a pure N_2 ice layer: it is therefore reasonable to assume that some N_2 becomes segregated in a layer separated from the remaining ice mixture upon heating. For this segregated fraction of N_2, $R_{BE} = 0.893 \pm 0.003$, due to the rise in the mean desorption energy of CO; for the remainder of the N_2, $R_{BE} = 1$.

4. DISCUSSION

The results from these experiments, summarized in Figure 3, have a direct impact on the modeling of CO and N_2 desorption in prestellar and star-forming cores. First, since the desorption behavior of layered and mixed ices is not identical, a decision has to be made on which of these systems most suitably emulates the interstellar case. Second, the desorption kinetics of CO and N_2 should be modeled as zeroth- and not first-order processes, with adopted rates independent of the surface concentration of the molecules, with preexponential factors in the rate constant of 10^{28}–10^{32} molecules cm^{-2} s^{-1} (Fraser et al. 2001; Collings et al. 2003a). Depending on the initial ice morphology and assuming that depleted molecules play no part in any grain-surface chemistry, some fraction of the N_2 originally frozen-out on interstellar grains will only desorb as the CO multilayers themselves desorb.

Irrespective of the ice morphology, this work gives $E_b(N_2\text{-}N_2) = 790 \pm 25$ K and $E_b(N_2\text{-CO}) = 855 \pm 25$ K, except in the mixed ice, where $E_b(\text{CO-CO}) = 885 \pm 25$ K. Within experimental error, these values are consistent with those obtained by Collings et al. (2003a) but significantly smaller than the E_b(CO-CO) value of 960 K (Sandford & Allamandola 1990) used in BL97 or $E_b(\text{CO-SiO}_2)$ of 1210 K (Bergin et al. 2002). The latter value is closer to the experimentally determined value of $E_b(\text{CO-H}_2\text{O}) = 1180 \pm 20$ K (Collings et al. 2003b; Fraser et al. 2004). It is clear that the most suitable ratio between the binding energies of N_2 and CO, R_{BE}, is 0.923 ± 0.003 for all cases where N_2 desorbs from "pure" ice environments. However, $R_{BE} = 1$ for the fraction of N_2 that codesorbs with CO. The lowest empirical value of R_{BE}, 0.893 ± 0.003, is found in mixed ices, where the lower ratio reflects the rise in the mean value of E_b(CO-CO). Nevertheless, all these ratios are significantly greater than any of the values adopted by BL97, Bergin et al. (2002), or Aikawa et al. (2003). Such a situation mimics that explored at the end of BL97, where R_{BE} was set to 1, to study the effects of the N_2 binding energy on N_2H^+ depletion, which was then enhanced by 2 orders of magnitude. These new laboratory data, when applied to models of dense cores, will certainly decrease the anticorrelation between gas-phase CO and N_2H^+ abundances. The next step is clearly to address detailed modeling of the CO-N_2 desorption kinetics followed by empirical studies of the tertiary CO-N_2-H_2O ice system.

We are grateful for comments by J. Jørgensen and T. Bergin and funding from NOVA, the Dutch Research School for Astronomy, and an NWO Spinoza grant to E. F. v. D; K. I. Ö. is grateful to the summer undergraduate research fellowship program at Caltech for sponsoring her visit to Leiden.

REFERENCES

Aikawa, Y., Ohashi, N., & Herbst, E. 2003, ApJ, 593, 906
Attard, G., & Barnes, C. 1998, Surfaces (Oxford: Oxford Univ. Press)
Belloche, A., & André, P. 2004, A&A, 419, L35
Bergin, E. A., Alves, J., Huard, T., & Lada, C. J. 2002, ApJ, 570, L101
Bergin, E. A., Ciardi, D. R., Lada, C. J., Alves, J., & Lada, E. A. 2001, ApJ, 557, 209
Bergin, E. A., & Langer, W. D. 1997, ApJ, 486, 316 (BL97)
Caselli, P., Walmsley, C. M., Tafalla, M., Dore, L., & Myers, P. C. 1999, ApJ, 523, L165
Chiar, J. E., Gerakines, P. A., Whittet, D. C. B., Pendleton, Y. J., Tielens, A. G. G. M., Adamson, A. J., & Boogert, A. G. A. 1998, ApJ, 498, 716
Collings, M. P., Dever, J. W., Fraser, H. J., & McCoustra, M. R. S. 2003a, Ap&SS, 285, 633
Collings, M. P., Dever, J. W., Fraser, H. J., McCoustra, M. R. S., & Williams, D. A. 2003b, ApJ, 583, 1058
Di Francesco, J., André, P., & Myers, P. C. 2004, ApJ, 617, 425
Elsila, J., Allamandola, L. J., & Sandford, S. A. 1997, ApJ, 479, 818
Fraser, H. J., Collings, M. P., Dever, J. W., & McCoustra, M. R. S. 2004, MNRAS, 353, 59
Fraser, H. J., Collings, M. P., McCoustra, M. R. S., & Williams, D. A. 2001, MNRAS, 327, 1165
Fraser, H. J., & van Dishoeck, E. F. 2004, Adv. Space Res., 33, 14
Jørgensen, J. K. 2004, A&A, 424, 589
Jørgensen, J. K., Schöier, F. L., & van Dishoeck, E. F. 2004, A&A, 416, 603
Kramer, C., Alves, J., Lada, C. J., Lada, E. A., Sievers, A., Ungerechts, H., & Walmsley, C. M. 1999, A&A, 342, 257
Lide, D. R. 2002, CRC Handbook of Chemistry and Physics (82nd ed.; Boca Raton: CRC Press)
Notesco, G., & Bar-Nun, A. 1996, Icarus, 122, 118
Pagani, L., Pardo, J.-R., Apponi, A. J., Bacmann, A., & Cabrit, S. 2005, A&A, 429, 181
Pontoppidan, K. M., et al. 2003, A&A, 408, 981
Sadlej, J., Rowland, B., Devlin, J. P., & Buch, V. 1995, J. Chem. Phys., 102, 4804
Sandford, S. A., & Allamandola, L. J. 1990, Icarus, 87, 188
Sandford, S. A., Bernstein, M. P., Allamandola, L. J., Goorvitch, D., & Teixeira, T. C. V. S. 2001, ApJ, 548, 836
Tafalla, M., Myers, P. C., Caselli, P., Walmsley, C. M., & Comito, C. 2002, ApJ, 569, 815
Tielens, A. G. G. M., Tokunaga, A. T., Geballe, T., & Baas, F. 1991, ApJ, 381, 181
Walmsley, C. M., Flower, D. R., & Pineau des Forêts, G. 2004, A&A, 418, 1035
Woodruff, D. P., & Delchar, T. A. 1994, Modern Techniques of Surface Science (2nd ed.; Cambridge: Cambridge Univ. Press), chap. 9
Whittet, D. C. B., et al. 1998, ApJ, 498, L159